NASA TECHNICAL MEMORANDUM

NASA TM X-2765

NASA TM X-2765

PERFORMANCE OF GAS-LUBRICATED NONCONFORMING PIVOTED-PAD JOURNAL BEARINGS AND A FLEXIBLY MOUNTED SPIRAL-GROOVE THRUST BEARING

by Lloyd W. Ream

Lewis Research Center

Cleveland, Ohio 44135

NATIONAL AERONAUTICS AND SPACE ADMINISTRATION • WASHINGTON, D. C. • MAY 1973

1. Report No.	2. Government Accession No.	3. Recipient's Catalog No.
NASA TM X-2765		

4. Title and Subtitle	5. Report Date
PERFORMANCE OF GAS-LUBRICATED NONCONFORMING PIVOTED-PAD JOURNAL BEARINGS AND A FLEXIBLY MOUNTED SPIRAL-GROOVE THRUST BEARING	May 1973
	6. Performing Organization Code

7. Author(s)	8. Performing Organization Report No.
Lloyd W. Ream	E-7269
	10. Work Unit No. 503-35

9. Performing Organization Name and Address	11. Contract or Grant No.
Lewis Research Center National Aeronautics and Space Administration Cleveland, Ohio 44135	
	13. Type of Report and Period Covered
12. Sponsoring Agency Name and Address	Technical Memorandum
National Aeronautics and Space Administration Washington, D.C. 20546	14. Sponsoring Agency Code

15. Supplementary Notes

16. Abstract

A test program was conducted to determine the performance characteristics of gas-lubricated nonconforming pivoted-pad journal bearings and a spiral-groove thrust bearing designed for the Brayton Cycle Rotating Unit (BRU). Hydrostatic, hybrid (simultaneously hydrostatic and hydrodynamic), and hydrodynamic tests were conducted in argon gas at ambient pressure and temperature ranges representative of hydrostatic operation up to the 10.5-kWe BRU power-generating level. Performance of the gas lubricated bearings is presented, including hydrostatic gas flow rates, bearing clearances, bearing temperatures, and transient performance.

17. Key Words (Suggested by Author(s))	18. Distribution Statement
Brayton rotating unit; Pivoted pad gas bearings; Spiral groove thrust bearing; Flexure instability	Unclassified - unlimited

19. Security Classif. (of this report)	20. Security Classif. (of this page)	21. No. of Pages	22. Price*
Unclassified	Unclassified	27	$3.00

* For sale by the National Technical Information Service, Springfield, Virginia 22151

PERFORMANCE OF GAS-LUBRICATED NONCONFORMING PIVOTED-PAD JOURNAL BEARINGS AND A FLEXIBLY MOUNTED SPIRAL-GROOVE THRUST BEARING

by Lloyd W. Ream

Lewis Research Center

SUMMARY

A test program was conducted to determine the performance characteristics of gas-lubricated nonconforming pivoted-pad journal bearings and a spiral-groove thrust bearing designed for the Brayton Cycle Rotating Unit (BRU). Hydrostatic, hybrid (simultaneously hydrostatic and hydrodynamic), and hydrodynamic tests were conducted in argon gas at ambient pressure and temperature ranges representative of hydrostatic operation to the 10.5-kWe BRU power-generating level. The first phase of testing of these gas bearings was to determine the hydrostatic performance of the jacking gas flow and the lift capability. The required total flow to the bearings is 7.33 grams per second (16.16×10^{-3} lb/sec) at 6-kWe ambient conditions. During hydrostatic operations, lifting of the shaft away from the bearings occurred when the ratio between supply pressure and ambient pressure exceeded a value of 4.25 also at the 6-kWe ambient conditions. The second phase of testing was to operate the bearings in a hybrid mode to locate the critical speed and instabilities. The largest orbit diameter obtained was 24 micrometers (0.00095 in.) at 8600 rpm. At 36 000 rpm the thrust bearing flexure proved to be unstable as the result of a self-excited oscillation of one-half synchronous frequency, thereby limiting the testing of the thrust bearing. The third phase of the testing was to operate the bearings hydrodynamically at the 6-kWe power level to measure their self-acting behavior at rated speed. The gas film of the journal bearings was 13 micrometers (0.0005 in.), and the maximum circular orbit at the compressor-bearing end of the shaft was 4.5 micrometers (0.00018 in.) in diameter. In the hydrodynamic mode the steady-state temperature reached by the bearings is comparable to the temperature reached in a hot BRU.

INTRODUCTION

The NASA Lewis Research Center is investigating the technology of the Brayton cycle system for electrical power generation. As part of the supporting bearing program, alternate gas bearings were designed and fabricated by Mechanical Technology Incorporated of Latham, New York; and they are fully described in reference 1. These bearings were installed at Lewis in a Brayton Rotating Unit (BRU) dynamic simulator and experimentally evaluated.

Reference 2 describes the power system for which the Brayton Rotating Unit and the alternate bearings are designed. Reference 3 describes the BRU dynamic simulator, in which the bearings were installed and tested. Basically, the tests were made to determine the bearing loading performance. Argon was used as the bearing lubricant, while air was used to drive the turbine.

Three modes of testing were used for this bearing evaluation. The first mode - hydrostatic - is applying jacking gas to the bearings, controlling the housing pressure, and allowing zero rotation of the rotor. The second mode - hybrid - is adding rotor rotation to the hydrostatic mode, achieved by spinning up the rotor to rated speed with the air-driven turbine. The third mode - hydrodynamic - is self-acting operation. This mode of operation of the bearings was accomplished by slowly removing the jacking gas supply from the bearings until they operated on the gas film that they themselves generated.

This report presents the findings of these various tests. Because of a thrust-bearing flexure instability, the thrust bearing was not run hydrodynamically and consequently was not evaluated in this respect.

Although the primary units are given in the SI system, the work was performed in the U.S. customary system.

BEARING DESIGN

The conditions under which the gas bearings were designed to operate are as follows:

Rotor speed, rpm	36 000
Rotor weight, kg (lb)	9.9 (21.8)
Lubricant	Helium-xenon (molecular weight, 83.8)
Viscosity, N-sec/m^2 (poise)	3.52×10^{-5} at 172° C (3.52×10^{-4} at 340° F)
Bearing cavity ambient pressure, N/cm^2 abs (psia)	6.8 to 29 (10 to 42.6)
Bearing cavity ambient pressure at 6 kWe, N/cm^2 abs (psia)	17.8 (25.8)

Journal Bearing

The nonconforming pivoted-pad journal bearing has the following geometric properties:

Journal diameter at 21° C (70° F) at 0 rpm, cm (in.)	4.4439 (1.7496)
Pad diameter at 21° C (70° F), cm (in.)	4.4562 (1.7544)
Pad length, cm (in.)	3.33 (1.312)
Pad arc length, rad (deg)	1.92 (110)
Pivot position (ratio)	0.65
Pivot diameter, cm (in.)	0.9525 (0.375)
Pivot seat diameter, cm (in.)	1.0 (0.3937)
Flexure stiffness, kg/cm (lb/in.)	360 (2000)

The gas-lubricated journal bearings are of the three-segment, pivoted-pad type which are shown in figure 1. An external pressurization orifice is provided at each pad pivot to permit operation of the journal bearing during startup and shutdown.

Each of the three equally spaced pads in each journal bearing is pivoted on a ball and a spherical seat. An exploded view of a pad and pivot is shown in figure 2. The pivot location is 65 percent of the pad length from the leading edge. The pads are made of AISI 416 steel hardened to 26 to 32 Rockwell C. The pivot consists of a nonconforming sliding-contact ball and spherical seat both of which are made of M-1 tool steel and are shown in figure 3. Included in the journal bearing design is provision for hydrostatic lift-off of each pad during startup, slow-speed operation, and shutdown. Hydrostatic lift-off is obtained by pressurizing a single hydrostatic orifice in each pad with jacking gas. Two of the pivot rods in each bearing are attached to solid beams shown in figures 1 and 4 and are rigidly attached to the frame by means of the bearing carrier shown in figure 4. The third pivot rod is mounted to the frame by means of the bearing carrier through a resilient beam with a nominal spring rate of 360 kilograms per centimeter (2000 lb/in.) also shown in figures 1 and 4. At assembly, shims are installed between the resilient beam and the bearing carrier so that the bearing pad is preloaded against the shaft. The shaft is clamped between the three pads with a preload of 16 to 23 newtons (8 to 12 lb). The low spring rate (360 kg/cm, or 2000 lb/in.) is used to accommodate differential growth, which tends to change bearing clearance. The growth is caused by thermal as well as centrifugal forces. Normal bearing ambient gas supply required to maintain the lubricant to the gas bearing is supplied by a bleed flow from the compressor discharge. The flow of the gas bleed is controlled by labyrinth seals at the turbine and compressor wheels sized to limit the total bleed flow to 2 percent of the compressor flow.

Thrust Bearing

The spiral-groove thrust bearing, shown in figure 5, has the following geometric properties:

Outside diameter, cm (in.)	10.80 (4.25)
Inside diameter, cm (in.)	5.3 (2.1)
Number of spiral grooves	18
Spiral angle, rad (deg)	1.27 (72.9)
Inner radius of groove annulus, cm (in.)	7.77 (3.06)
Groove-width to land-width ratio	1.6

The gas-lubricated thrust bearing is of the spiral-grooved type and is shown in figure 1. Externally pressurized orifices (too small to be seen in the photograph) are provided in each bearing stator plate to permit operation of the thrust bearing during startup and shutdown.

The thrust bearing design consists of two flat plates bolted together at the periphery and separated by a spacer that is 100 micrometers (0.004 in.) thicker than the thrust runner. The bearing stator plates are made of annealed AISI 416 steel and are coated with approximately 50 micrometers (0.002 in.) of chromium oxide. The bearing surface of each plate contains 18 spiral grooves which are formed by masking the surface and then plasma spraying with chromium oxide.

Flexure

The thrust bearing assembly is flexibly supported, by four spokes, from an outer member which locates and attaches the bearing assembly to the housing. The four-spoke flexible-support member shown in figures 1 and 6 is a furnace-brazed subassembly consisting of an inner ring joined to an outer ring by brazing the spokes to that ring. To prevent buckling of the spokes due to differential expansion, they are positioned tangentially to the inner and outer rings. With this configuration, differential expansion causes the inner ring to rotate relative to the outer ring, a motion which is acceptable to the design.

The angular stiffness of the flexure assembly is 220 N-m/rad (38 900 in.-lb/rad), approximately one-third of the tilt stiffness of the gas film at load condition of 63 newtons (31 lb). With this stiffness the flexure can accommodate 75 percent of the misalinement that may exist between the thrust rotor and stator. However, this feature also results in a flexibility in the axial direction which is undesirable from the standpoint of retention of the axial clearance between the turbine and compressor wheels and their housings.

APPARATUS

BRU Dynamic Simulator

The basic function of the BRU Dynamic Simulator is to provide a vehicle for subjecting the gas bearing/rotor suspension system to the same mechanical, electromagnetic, and thermal conditions expected in the actual BRU loop operation.

The dynamic simulator shown in cross section in figure 7 is identical to the BRU, with the exception of dummy wheels which have the masses of the turbine and compressor wheels. The compressor dummy wheel also functions as the drive turbine, with its drive-turbine housing replacing the BRU compressor scroll. Figures 4 and 8 show the turbine and compressor bearing ends, respectively, of the dynamic simulator prior to installation of the air-drive turbine housing and shroud and the turbine dummy wheel. A more complete description of the BRU dynamic simulator may be found in reference 3.

Schematic drawings of the cold-spin facility and the jacking gas system are shown in figures 9 and 10, respectively. Pressurization is provided on the back surface of the compressor dummy wheel at prescribed levels to effect desired axial loadings on the thrust bearing. The rim of the dummy wheel is an effective seal between the turbine drive air and the thrust loading cavity. The cavity between the BRU labyrinth seal and the rim seal on the dummy wheel is pressure controlled to ensure leakage of process gas from the bearing cavity. This leakage flow path is physically representative of that of the BRU and also precludes contamination of the bearing cavity caused by any possible adverse flow from the air-drive turbine. A small amount of pressure-regulated argon is fed into the alternator housing. The amount of argon is equivalent to the compressor bleed flow, which is the gas supply to the bearings for hydrodynamic operation.

Bearing Jacking Gas System

The bearing jacking gas system provides external pressurization to the journal and thrust bearings for starting up, stopping, and emergency operation. This system is shown schematically in figure 10. Each bearing is supplied with 103 N/cm^2 abs (150 psia) of argon gas from a separate regulator which is closed off manually for hydrodynamic operation. An emergency pressure regulator was provided parallel with the working regulator and isolated by a solenoid valve. During hydrodynamic operation, if the speed dropped below a preset value, the solenoid valve opened to provide external pressurization to the bearings.

Instrumentation

Chromel-Alumel thermocouples are used for the measurement of the temperature of the bearing parts. A total of two thermocouples are associated with one complete set of bearing parts and are located as follows:

(1) Journal bearings

(a) One thermocouple located adjacent to the pivot on each bearing pad

(b) Four thermocouples on the loaded pad of each bearing located at the leading edge, at the trailing edge, and on each side

(c) Three thermocouples equally spaced around each journal bearing support

(2) Thrust bearing: Two thermocouples on the back, or nonactive side, of each thrust stator (The thermocouples are equally spaced and located along a radial line extending from the inside diameter to the outside diameter of the bearing.)

The measurement of static and dynamic film thicknesses and the measurement of dynamic motion of the bearing components is accomplished by using a displacement measuring system. This system measures the capacitance of the space between the tip of a transducer and the surface under observation. Measurement of thrust film thickness is made by using three equally spaced capacitance probes located in the thrust plate adjacent to the compressor wheel location shown in figure 11. Another capacitance probe is used to measure film thicknesses in the thrust bearing adjacent to the journal bearing. In addition to measuring the thrust bearing film thickness, two capacitance probes measure the dynamic motion of the thrust stator relative to the housing.

The journal bearing film thickness is measured by a capacitance probe in the bearing pad located as close to the pivot point as the mechanical design allows, shown in figure 12. Also shown in figure 12 are the locations for the capacitance probes to measure the dynamic motion of the journal bearing pad. The pitch probe is located toward the leading edge of the pad and on the bearing centerline. The roll probe is located towards the end of the pad and in line with the pivot. Also, the pitch and roll probes can be used for measuring gas film thicknesses at their respective locations.

PROCEDURE

The initial step in testing the nonconforming pivoted-pad journal bearing and the spiral-groove thrust bearing was to establish the hydrostatic jacking gas flow characteristics of the bearings. Rotation was then started and gradually increased until the rated speed of 36 000 rpm was reached. At 36 000 rpm the hydrostatic jacking gas was gradually turned off, at which time the bearings were completely self-acting. During the removal of the jacking gas from the thrust bearing, the flexure exhibited an insta-

bility. The procedure was then changed to permit only the journal bearings to be run hydrodynamically. Once the journal bearings became self-acting, the housing pressure was adjusted for the 6-kWe power level and run for about 5 hours to reach thermal stability. The 6-kWe reference power level was used in this investigation to be consistent with the original BRU design specification. Off-design performance of the BRU was to range from 2.25- to 10.5-kW net electrical output based on a reference output design of 6 kWe.

DISCUSSION OF RESULTS

Hydrostatic Performance

Flow rate. - Design information for jacking gas systems is provided by measuring bearing gas flow rate at zero speed. The supply pressure to the bearings ranged from 69 to 103 N/cm^2 abs (100 to 150 psia) in increments of 6.8 N/cm^2 abs (10 psia) at constant temperature of 300 K (540^o R). The bearing cavity (simulator housing) pressure was regulated to three pressure levels - 9, 17, and 31 N/cm^2 abs (13.5, 25, and 45 psia) - at constant inlet temperature of 300 K (540^o R). Figure 13 is a plot of the gas flow to the turbine journal bearing over the range of bearing pressures tested for the two extremes in cavity pressure. At normal bearing supply pressure of 103 N/cm^2 abs (150 psia) and the simulated 6-kWe power level, the flow to the turbine journal bearing is 0.33 gram per second (0.73×10^{-3} lb/sec). Also shown on figure 13 are points where the bearing is free from the journal for the two extreme cavity pressure levels; at this condition the shaft can rotate. The argon gas flow is shown in figure 14 as it was determined for the thrust bearing, using the same supply pressure range that was used for the journal bearing. At the reference 6-kWe and normal thrust bearing gas supply pressure, the flow is 6.67 grams per second (1.47×10^{-2} lb/sec). Within the accuracy and the location of the instrumentation, no significant difference in flow to the thrust bearing was measured for the variations in the cavity pressure level covered in this test. The total flow of the thrust and journal bearings is presented in figure 15. At 103-N/cm^2 abs (150-psia) bearing supply pressure and the reference 6-kWe power level, the flow is 7.33 grams per second (16.16×10^{-3} lb/sec) measured at the inlet lines to the housing.

Associated with the jacking gas flow to the bearing is the requirement that the jacking gas source must supply and maintain a high enough gas pressure between the bearing pad and the shaft to lift the shaft off the bearing. Figure 16 is a plot of the pressure ratios that were required to get the shaft to lift off the bearings at the various housing pressures. Pressure ratio defined herein is the ratio of the bearing supply pressure to the housing pressure measured at the inlet fittings to the simulator housing. In this

plot the shaft will lift above the band. These data are good only for this particular build, that is, with 39-newton (8.8-lb) bearing preload. The bearing preload will vary from build to build because of the many variables that are involved in setting up the preload and will shift the level of the band.

Bearing film. - Measurements of hydrostatic film thickness as a function of bearing cavity (housing) pressure are presented in figure 17. For normal hydrostatic operation of 103-N/cm^2 abs (150-psia) bearing gas supply pressure and 17-N/cm^2 abs (25-psia) cavity pressure, the film thickness at a turbine fixed journal pad is approximately 15 micrometers (0.0006 in.).

The gas film between the thrust rotor and the compressor thrust stator is less than the gas film on the turbine side of the bearing. Figure 18 shows that in the hydrostatic operation and with the dynamic simulator set for the reference condition 103-N/cm^2 abs (150-psia) bearing supply pressure and the housing set to 6-kWe pressure level), the films are 33 micrometers (0.0013 in.) and 75 micrometers (0.00295 in.) for the compressor and turbine sides, respectively. The difference in the film is caused by the direction of the load. The primary hydrostatic load is the rotor weight only toward the compressor.

Hybrid Performance

Hybrid is defined herein as that condition under which the thrust and journal bearings are externally supplied with gas lubricant, the machine is running at some known speed, and the housing is pressurized.

Bearing transient performance. - During startup and shutdown, journal bearing critical speeds are encountered. The BRU is designed to pass through the first and second critical speeds and is to operate between the second and third critical speeds. In the critical speed regions, large increases occur in the shaft orbit. The orbit size depends upon the amount of shaft unbalance and on the rate of acceleration or deceleration. The largest orbits occur during shutdown because of the slow rate of deceleration.

Figure 19 shows the turbine and compressor orthogonal traces as displayed on the oscilloscopes during shutdown. The lower two oscilloscope traces (fig. 19(b)) give the critical speeds at approximately 7500 and 6700 rpm; the turbine and compressor shaft orbits are 11 and 22 micrometers (0.00045 and 0.0009 in.), respectively. The upper two oscilloscope traces (fig. 19(a)) are of critical speeds occurring at 11 500 and 8600 rpm for the turbine and compressor ends, respectively. The turbine orbit reaches maximum amplitude of 8 micrometers (0.00032 in.), and the compressor orbit reaches an amplitude of 24 micrometers (0.00095 in.).

Thrust bearing flexure. - The transient performance of the thrust bearing flexure was instable because of a self-excited oscillation of the flexure. As the external supply of gas to the thrust bearing was being reduced in pressure from the 103 N/cm^2 abs (150 psia) to zero, at about 48 N/cm^2 abs (70 psia) the motion of the flexure suddenly increased in amplitude with predominantly a one-half synchronous-frequency component.

The flexure motion relative to the housing is measured by capacitance probes W and X, the location of which is shown diagrammatically in figure 11. The motion of the flexure for the hybrid mode of operation is shown in figure 20(b). Shown in figure 20(a) is the relative motion of the compressor side of the thrust rotor (probe Q) relative to the motion of the flexure (probe X). The hybrid mode is stable with very little motion of the flexure relative to the housing and the thrust rotor. Figure 21 shows the oscilloscope traces of the flexure (probe W) relative to the thrust bearing rotor. Probe W was used since probe X malfuntioned. It shows the large amplitude of motion that appeared suddenly when the jacking gas pressure was reduced to 46 N/cm^2 abs (67 psia). A mechanical friction damper successfully used on the Rayleigh step thrust bearing has been designed to eliminate this instability and will be evaluated in the forthcoming test of the spiral-groove thrust bearing and another alternate journal bearing.

Hydrodynamic Performance

Bearing component motion. - During the transition period from hybrid to hydrodynamic operation, the oscilloscope traces showed no measurable change in size or waveform. Photographs of the bearing component oscilloscope traces were taken approximately 5 hours after the journal bearings were self-acting.

The compressor bearing orbit and its corresponding time-base trace are shown in figure 22(a). Each small vertical division of the grid is equal to 2.5 micrometers (0.0001 in.). The orbit is slightly elliptical with a major axis of 4.5 micrometers (0.00018 in.), which is consistent with other BRU and BRU simulator assemblies and is representative of the degree of unbalance.

The turbine bearing orbit is shown in figure 22(b). The orbit is circular with an axis of 2.5 micrometers (0.0001 in.). The time-base traces of both orthogonal probes C and D are sinusoidal.

The top trace (compressor probe) of figure 23 shows the motion of the leading edge of the compressor flexibly mounted pad. The amplitude is 2.5 micrometers (0.0001 in.) and is sinusoidal. The bottom trace (turbine probe) shows the motion of the leading edge of the turbine flexibly mounted pad. The motion of the pad appears to be out of the range of the capacitance probe.

Figure 24(a) shows the gas film of one of the fixed mounted turbine pads measured at the pivot line of the pad; its location is shown schematically in figure 12. The grid marked E = 0 is the output value of the E probe when the shaft is at rest and in contact with the turbine journal pad. The vertical distance from the datum line (E = 0) to the oscilloscope trace is the measurement of the gas film thickness at the pivot line of the pad and is 13 micrometers (0.005 in.).

The traces shown in figure 24(b) are roll motions of the flexibly mounted pads. Roll motion is tilting of the pad in the direction of the axis of the shaft and is fully described in reference 3. The top trace is the motion of the compressor journal pad, and the bottom traces are the motion of the turbine pads. The roll motion of the bearing pads is small and considered to be insignificant.

Bearing temperatures. - The bearing temperatures reached in the simulator during ambient testing generally closely match the temperatures obtained during hot operation of an actual BRU at the 6-kW power level. Table I describes the location of the thermocouples used and the temperatures measured for these locations during the cold-spin test, along with a few actual temperatures recorded from a hot BRU operation reported in references 4 and 5. The maximum temperatures were on the turbine journal bearing and are of the same order of magnitude as the temperatures for the hot BRU operation.

CONCLUDING REMARKS

The flexible bearing support, chosen for its lack of wearing parts, is also lacking in the damping required for stable operation of the spiral-groove thrust bearing. Friction dampers have been used successfully on the Rayleigh step thrust bearing. Although such dampers might also stabilize the spiral-groove thrust bearing, the friction dampers were not tested in this investigation.

SUMMARY OF RESULTS

The results of cold-spin testing of nonconforming pivoted-pad journal bearings and a spiral-groove thrust bearing designed as alternate bearings for the BRU are summarized as follows:

1. The performance of the nonconforming pivoted-pad journal bearing was similar to that of the prototype fully conforming pivoted-pad journal bearing at the 6-kWe power level.

2. During the transition period from hydrid to hydrodynamic operation, the oscilloscope traces of the journal bearing motion showed no measurable changes in the size of the motion or in the wave shape.

3. At rated speed the largest shaft orbit diameter was approximately 4.5 micrometers (0.00018 in.).

4. Gas film thickness of the fixed turbine pad was 13 micrometers (0.005 in.) at rated speed.

5. The thrust bearing was instable at rated speed and could not be evaluated in the hydrodynamic mode.

6. The temperature distribution for the bearing system was found to be essentially the same as that of a hot Brayton Cycle Rotating Unit.

Lewis Research Center,
National Aeronautics and Space Administration,
Cleveland, Ohio, January 11, 1973,
503-35.

REFERENCES

1. Waldron, W. D.: Design and Fabrication of Gas Bearings for Brayton Cycle Rotating Unit. NASA CR-121098, 1973.

2. Klann, John L.: 2 to 10 Kilowatt Solar or Radioisotope Brayton Power System. Proceedings of the Intersociety Energy Conversion Engineering Conference. Vol. 1. IEEE, 1968, pp. 407-415.

3. Davis, J. E.: Design and Fabrication of the Brayton Rotating Unit. NASA CR-1870, 1972.

4. Klassen, Hugh A.; Winzig, Charles H.; Evans, Robert C.; and Wong, Robert Y.: Mechanical Performance of a 2- to 10-Kilowatt Brayton Rotating Unit. NASA TM X-2043, 1970.

5. Johnsen, Roy L.; Namkoong, David; and Edkin, Richard A.: Steady-State Temperature Distribution Within Brayton Rotating Unit Operating in a Power Conversion System Using Helium-Xenon Gas. NASA TM X-67990, 1971.

TABLE I. - COLD-SPIN-TEST THERMOCOUPLE LOCATIONS

AND TEMPERATURE MEASUREMENTS

Thermocouple	Location	Temperature			
		Ambient testing		Actual	
		°C	°F	°C	°F
25	Turbine bearing carrier	131	268	136	277
26	Turbine bearing carrier	132	270	136	278
29	Compressor bearing carrier	[a]26	[a]80	109	229
30	Compressor bearing carrier	115	239	112	234
	Turbine journal bearing				
38	Inboard edge D-shoe	158	317	---	---
39	Trailing edge D-shoe (film)	162	323	175	348
40	Outboard edge D-shoe	164	326	---	---
41	Leading edge D-shoe (film)	125	256	---	---
42	Inboard edge D-shoe	162	324	---	---
43	Inboard edge F-shoe	162	323	176	349
	Compressor journal bearing				
44	Inboard edge A-shoe	143	290	---	---
45	Trailing edge A-shoe (film)	146	294	144	291
46	Outboard edge A-shoe	147	296	---	---
47	Leading edge A-shoe	146	295	---	---
48	Inboard edge B-shoe	146	295	141	289
49	Inboard edge C-shoe	(a)	(a)	---	---
	Thrust bearing				
50	Thrust bearing spacer	126	259	165	329
51	Thrust bearing spacer	[a]26	[a]80	164	328
52	Turbine thrust bearing stator (in)	114	244	---	---
53	Turbine thrust bearing stator (mid)	124	245	---	---
54	Turbine thrust bearing stator (out)	125	256	---	---
55	Compressor thrust bearing stator (out)	129	264	---	---
56	Compressor thrust bearing stator (mid)	129	264	---	---
57	Compressor thrust bearing stator (in)	26	[a]80	---	---

[a]Defective thermocouple.

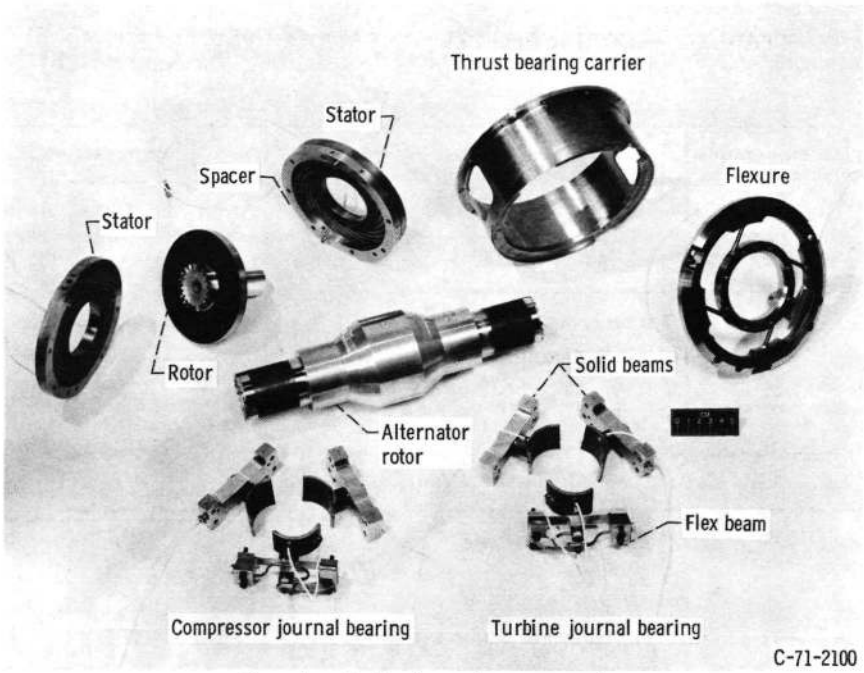

Figure 1. - Gas bearing system components.

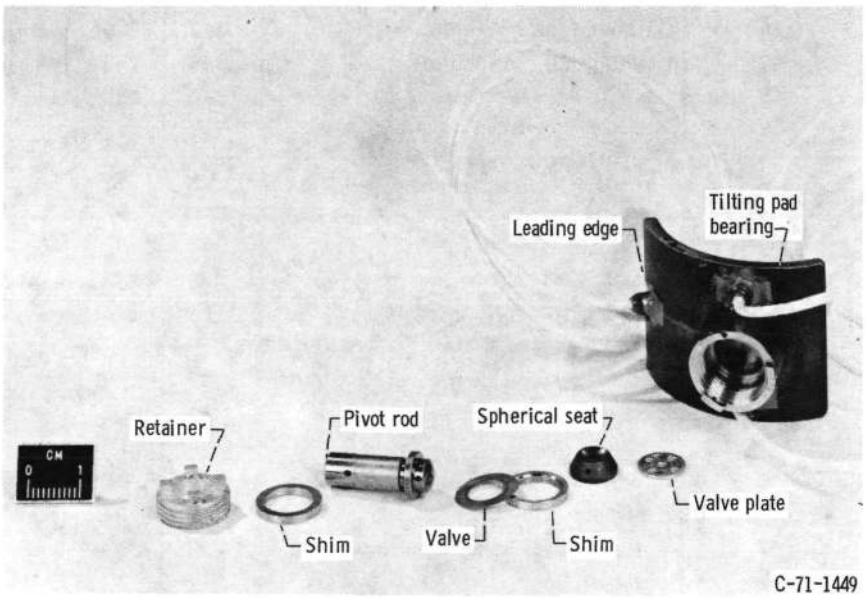

Figure 2. - Exploded view of nonconforming pivot pad.

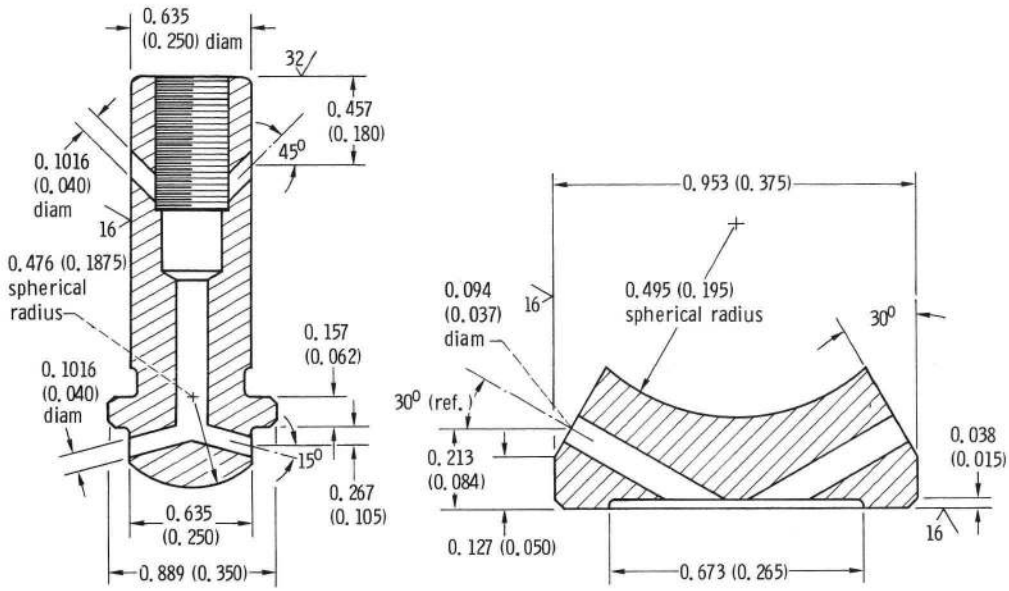

Figure 3. - Pivot. (Dimensions are in cm (in.).)

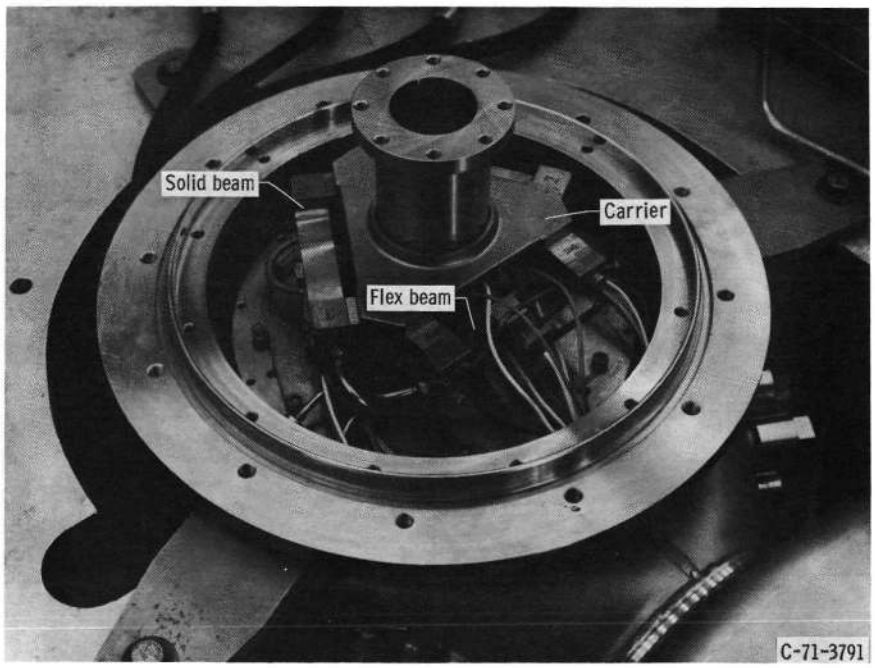

Figure 4. - Journal bearing installed in simulator.

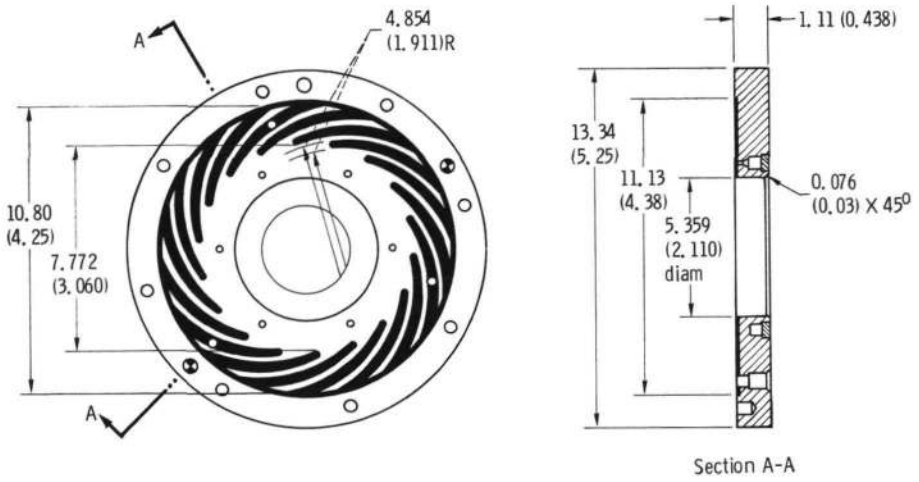

Figure 5. - Thrust stator. (Dimensions are in cm (in.).)

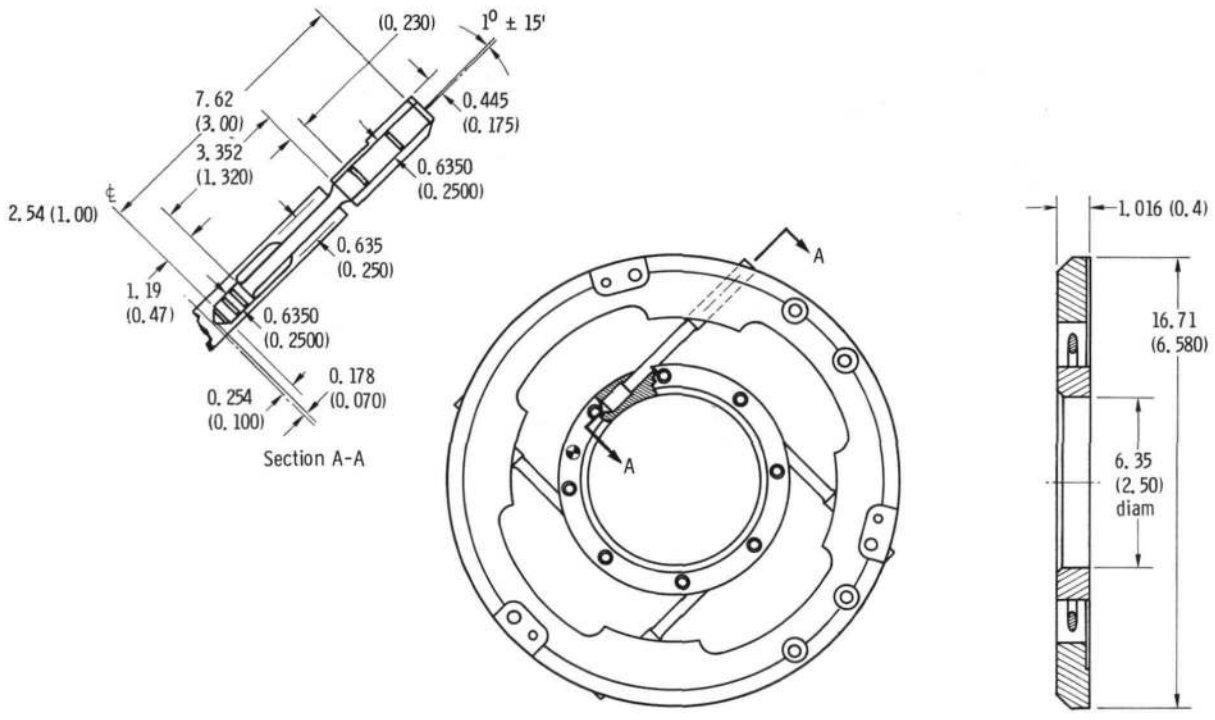

Figure 6. - Thrust bearing flexure mount. (Dimensions are in cm (in.).)

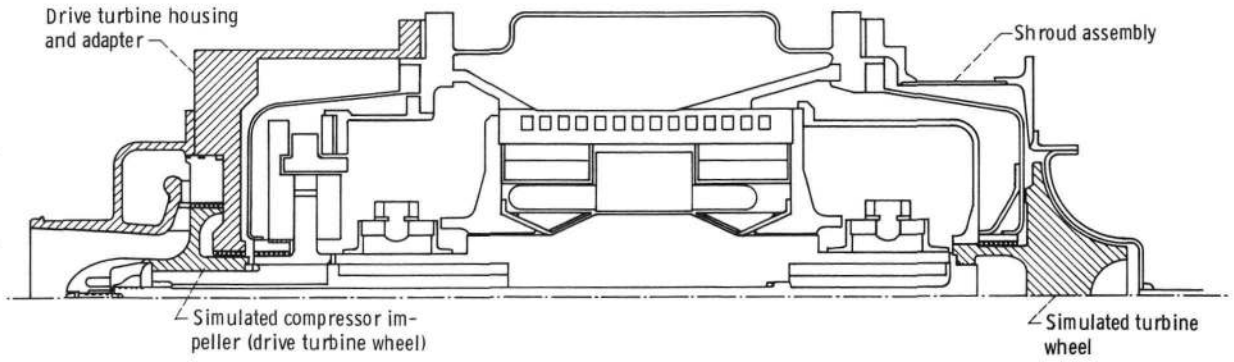

Figure 7. - Brayton Cycle Rotating Unit (BRU) dynamic simulator.

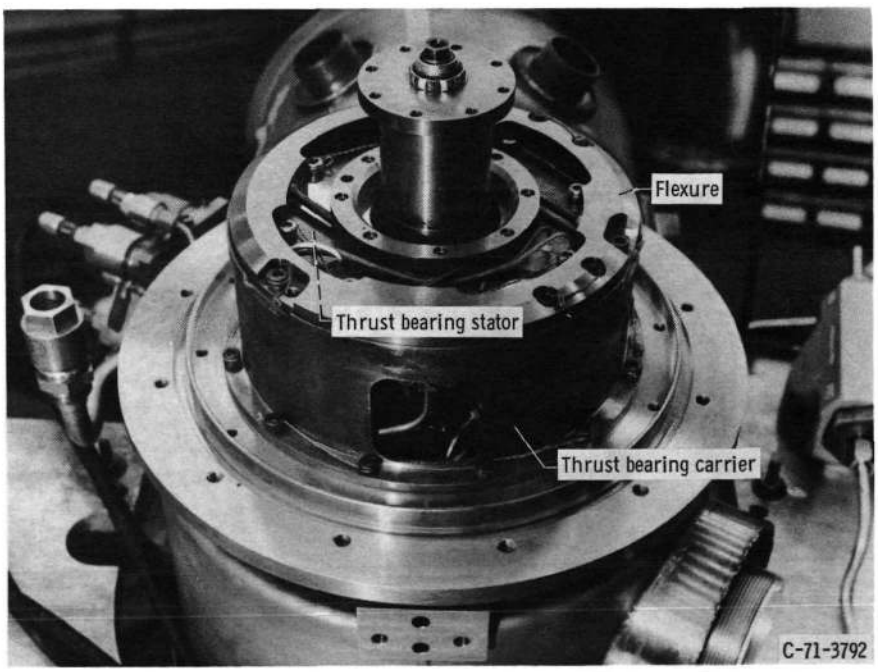

Figure 8. - Thrust bearing installed in simulator.

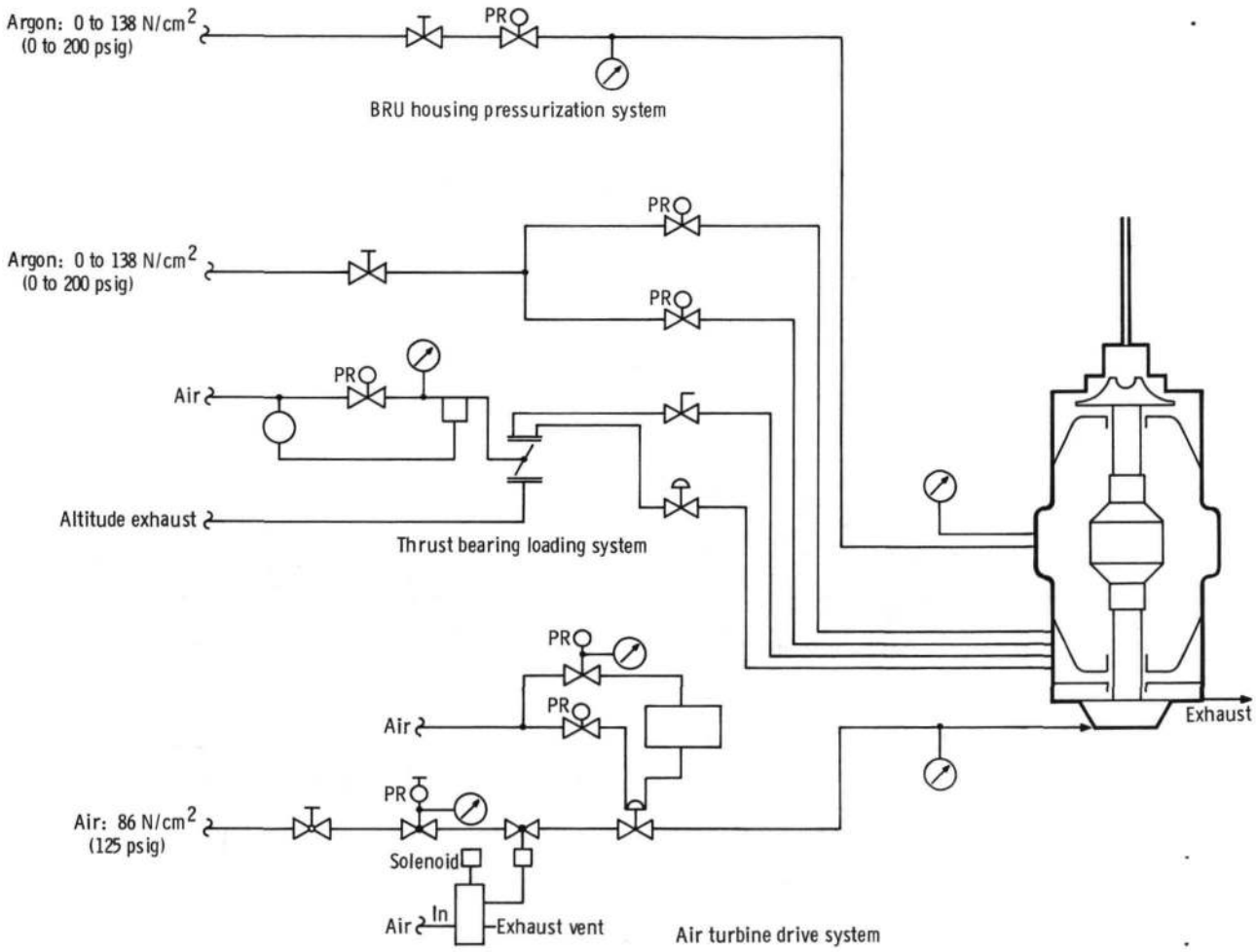

Figure 9. - Schematic drawing of cold-spin facility.

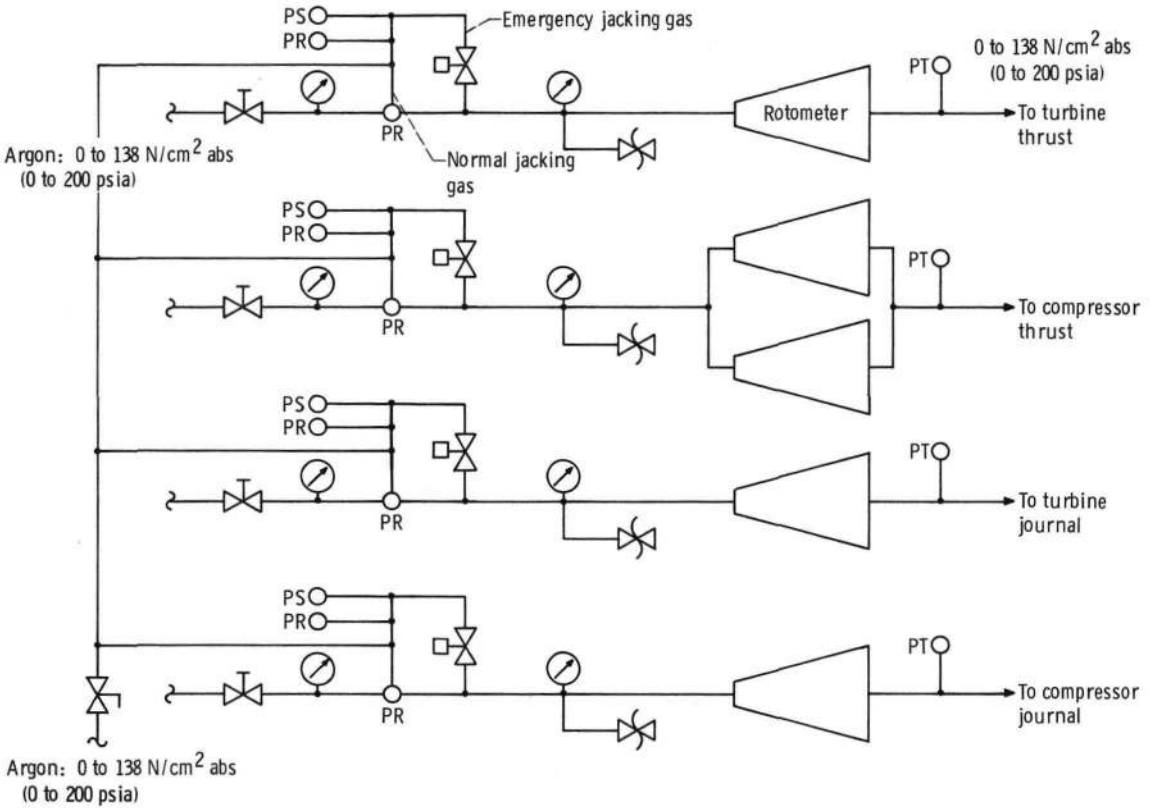

Figure 10. - Schematic drawing of jacking gas system.

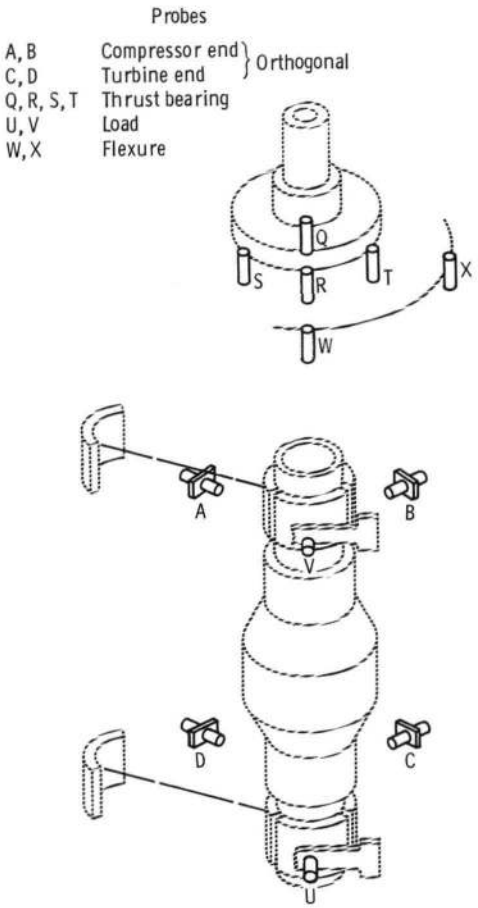

Figure 11. - Location of capacitance probes on thrust bearing, flex beams, and shaft orthogonals.

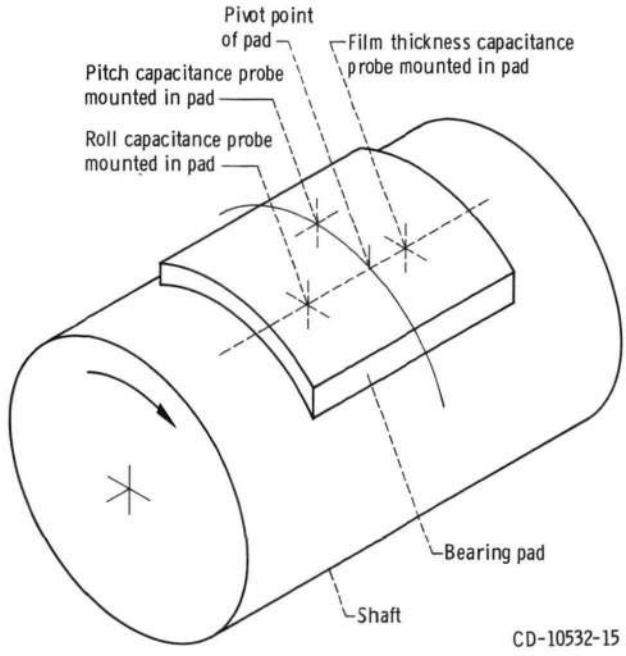

Figure 12. - Location of bearing capacitance probes on typical fully instrumented journal bearing pad.

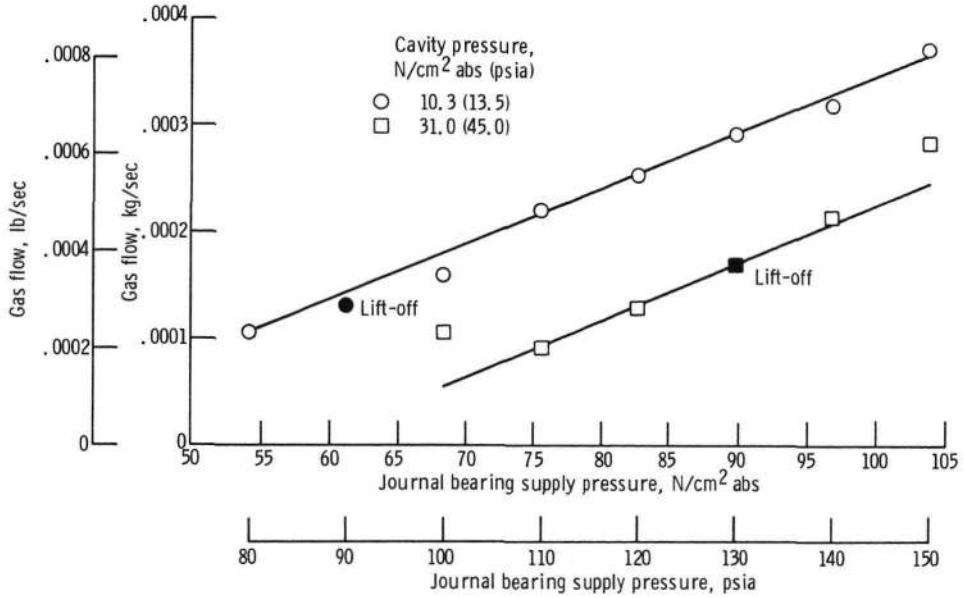

Figure 13. - Gas flow to turbine journal bearing.

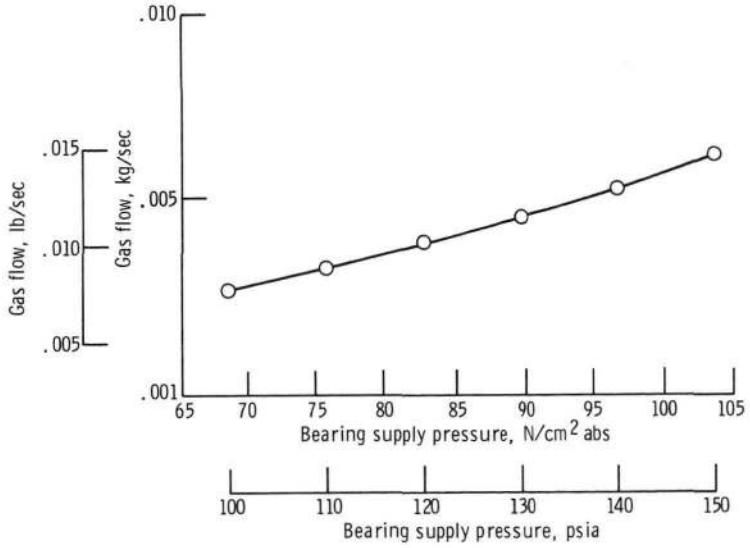

Figure 14. - Total gas flow to thrust bearing.

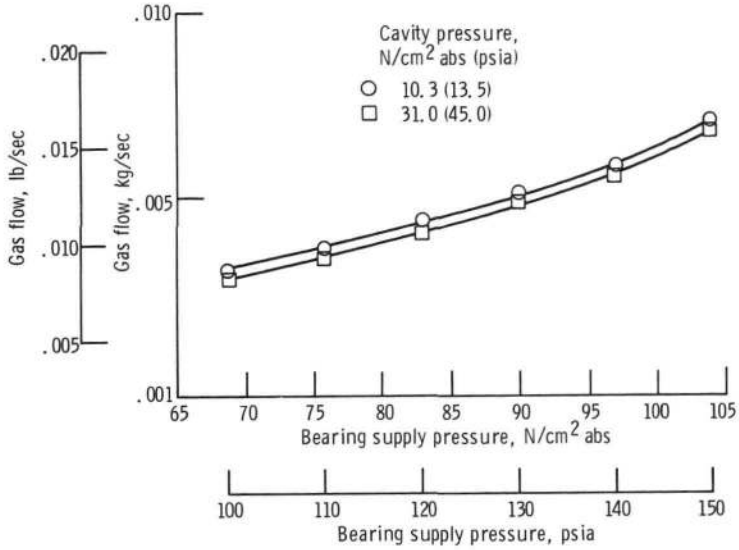

Figure 15. - Total gas flow to bearings.

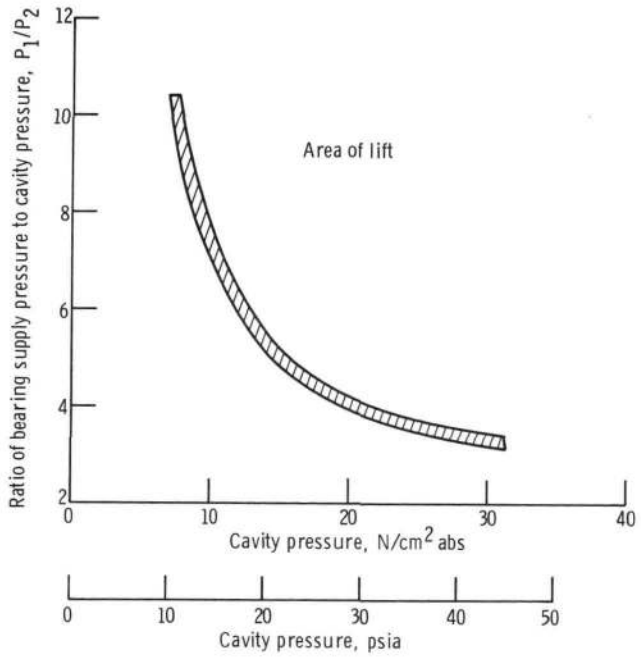

Figure 16. - Hydrostatic lift-off of nonconforming pivoted-pad journal bearing.

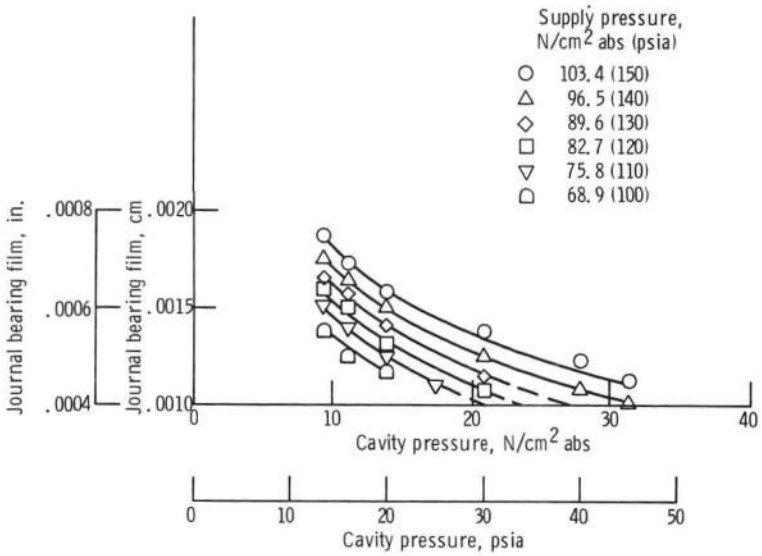

Figure 17. - Hydrostatic journal bearing film.

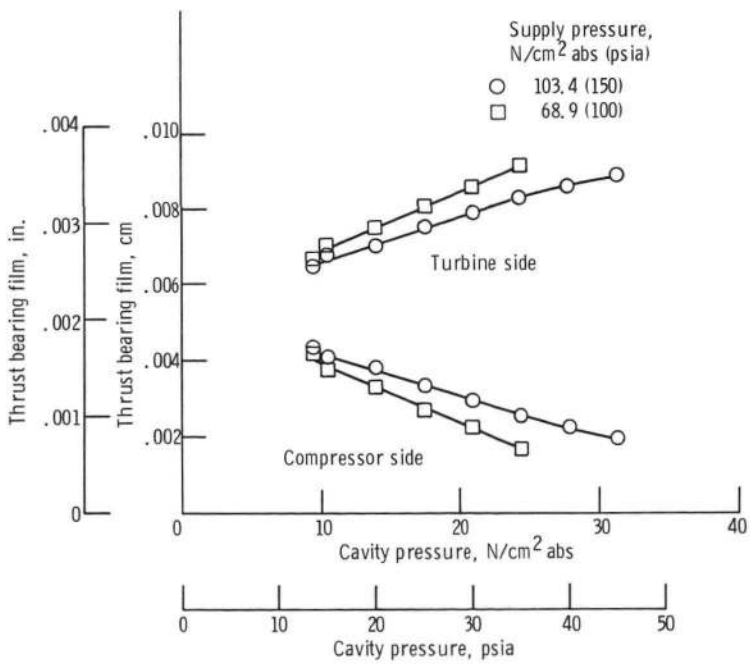

Figure 18. - Hydrostatic thrust bearing film.

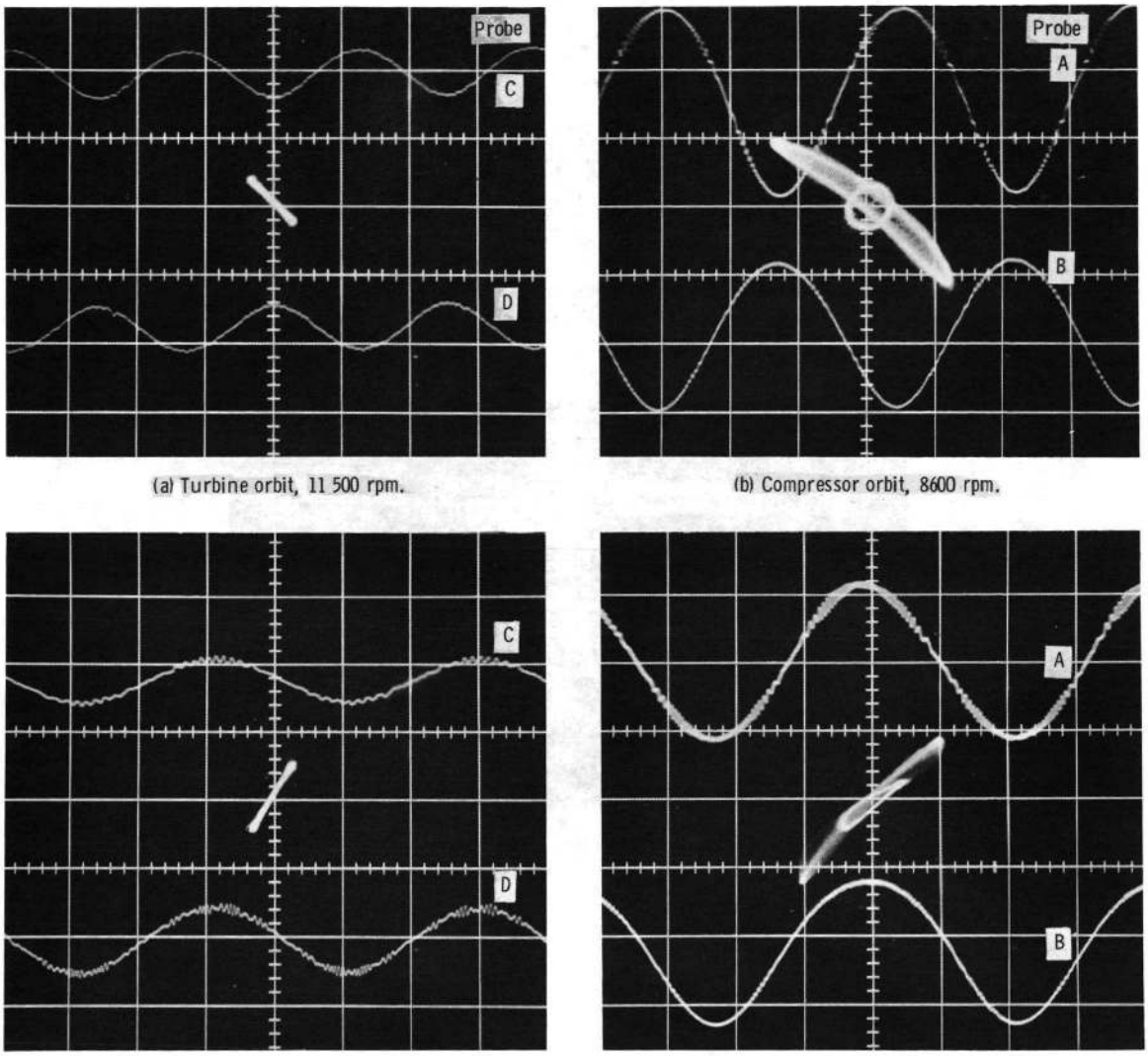

(a) Turbine orbit, 11 500 rpm.

(b) Compressor orbit, 8600 rpm.

(c) Turbine orbit, 7500 rpm.

(d) Compressor orbit, 6700 rpm.

Figure 19. - Critical speed. Cavity pressure, 17.3 N/cm^2 abs (25 psia); thrust bearing supply pressure, 103.4 N/cm^2 abs (150 psia); journal bearing supply pressure, 103.4 N/cm^2 abs (150 psia). Time scale, 2 milliseconds per centimeter; vertical scale, 0.25x10^{-3} centimeter (0.1 mil) per division .

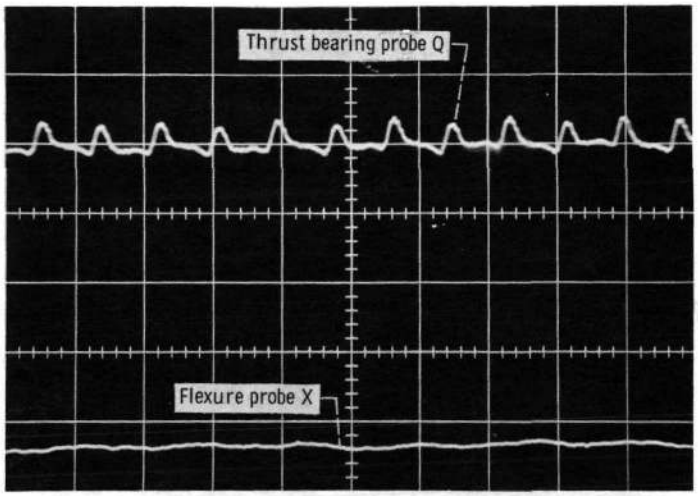

(a) Thrust bearing and flexure motion.

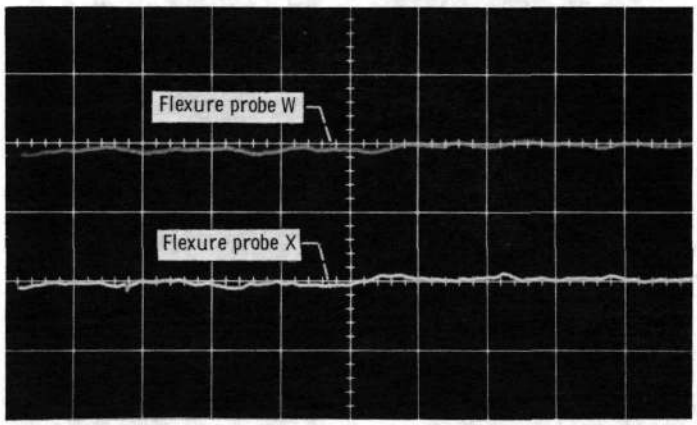

(b) Flexure motion.

Figure 20. - Thrust bearing and flexure motion. Cavity pressure, 17.3 N/cm^2 abs (25 psia); thrust bearing supply pressure, 103.4 N/cm^2 abs (150 psia); journal bearing supply pressure, 103.4 N/cm^2 abs (150 psia); speed, 36 000 rpm. Time scale, 2 milliseconds per centimeter; vertical scale, 0.25×10^{-3} centimeter (0.1 mil) per division.

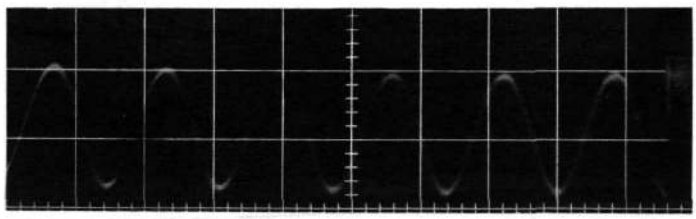

Figure 21. - Thrust bearing flexure instability - flexure probe W. Cavity pressure, 17.3 N/cm^2 abs (25 psia); thrust bearing supply pressure, 46 N/cm^2 abs (67 psia); journal bearing supply pressure, 103.4 N/cm^2 abs (150 psia); speed, 36 000 rpm. Time scale, 2 milliseconds per centimeter; vertical scale, 0.005 centimeter (2 mil) per major division.

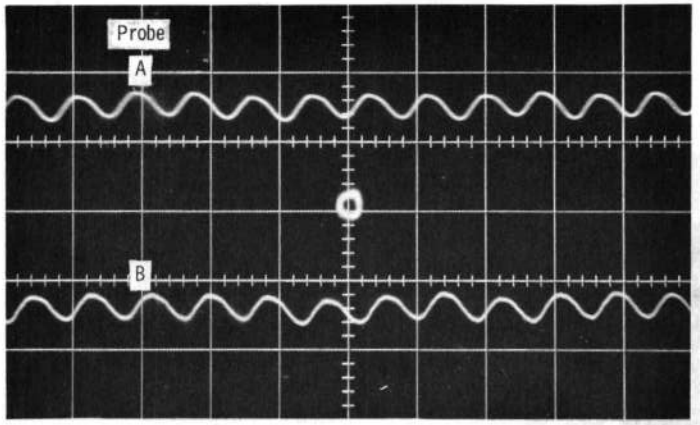

(a) Compressor journal bearing orbit.

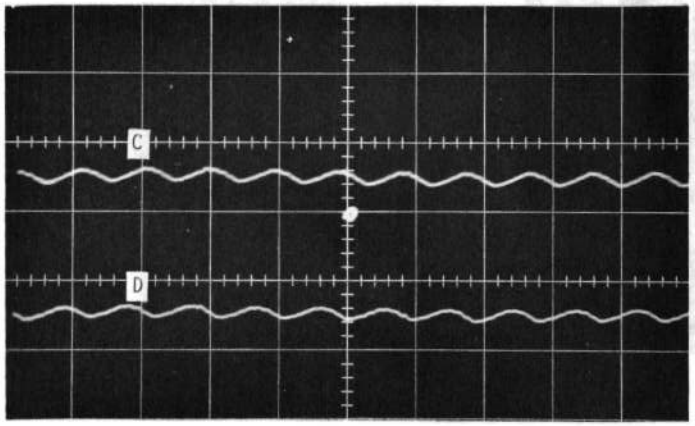

(b) Turbine journal bearing orbit.

Figure 22. - Shaft motion. Cavity pressure, 17.3 N/cm^2 abs (25 psia); thrust bearing supply pressure, 103.4 N/cm^2 abs (150 psia); self-acting journal bearing; speed, 36 000 rpm. Time scale, 2 milliseconds per centimeter; vertical scale, 0.25×10^{-3} centimeters (0.1 mil) per division.

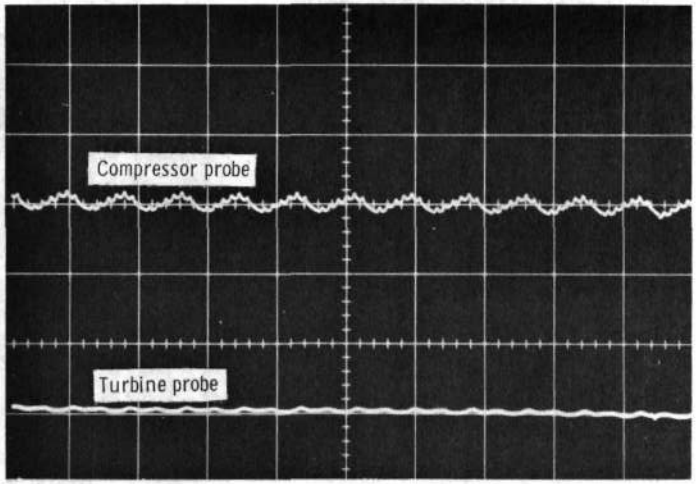

Figure 23. - Motion of leading edge of flexibly mounted journal bearing pads. Cavity pressure, 17.3 N/cm^2 abs (25 psia); thrust bearing supply pressure, 103.4 N/cm^2 abs (150 psia); self-acting journal bearings; speed, 36 000 rpm. Time scale, 2 milliseconds per centimeter; vertical scale, 0.25×10^{-3} centimeter (0.1 mil) per division.

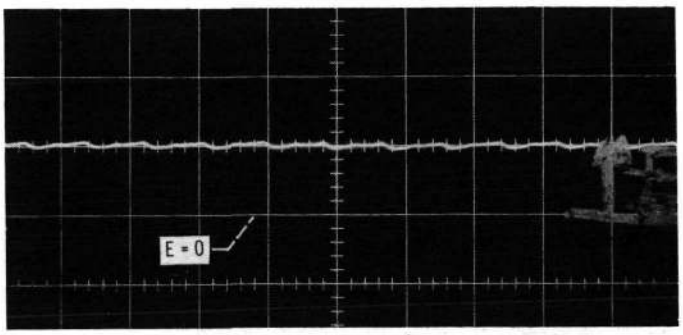

(a) Turbine journal bearing film.

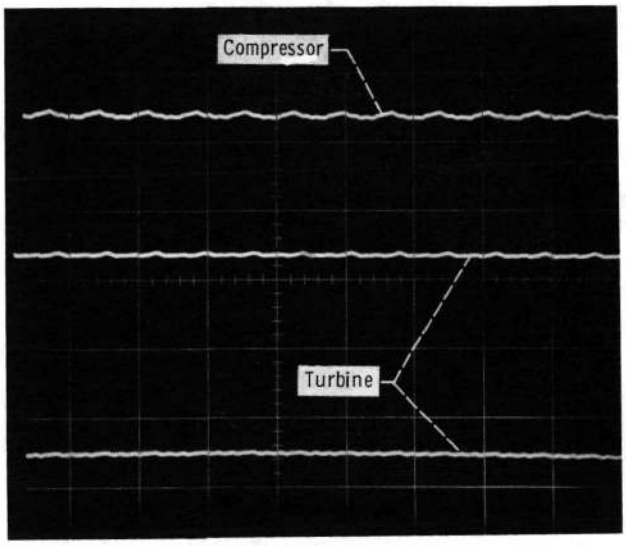

(b) Journal bearing roll motion.

Figure 24. - Journal bearing motion. Cavity pressure, 17.3 N/cm^2 (25 psia); thrust bearing pressure, 103.4 N/cm^2 abs (150 psia); self-acting journal bearings; speed, 36 000 rpm. Time scale, 2 milliseconds per division; vertical scale, 0.25×10^{-3} centimeter (0.1 mil) per division.

NASA-Langley, 1973 —— 3 E-7269

NATIONAL AERONAUTICS AND SPACE ADMINISTRATION
WASHINGTON, D.C. 20546

OFFICIAL BUSINESS
PENALTY FOR PRIVATE USE $300

SPECIAL FOURTH-CLASS RATE
BOOK

POSTAGE AND FEES PAID
NATIONAL AERONAUTICS AND
SPACE ADMINISTRATION
451

U.S.MAIL

POSTMASTER: If Undeliverable (Section 158 Postal Manual) Do Not Return

"The aeronautical and space activities of the United States shall be conducted so as to contribute . . . to the expansion of human knowledge of phenomena in the atmosphere and space. The Administration shall provide for the widest practicable and appropriate dissemination of information concerning its activities and the results thereof."

—NATIONAL AERONAUTICS AND SPACE ACT OF 1958

NASA SCIENTIFIC AND TECHNICAL PUBLICATIONS

TECHNICAL REPORTS: Scientific and technical information considered important, complete, and a lasting contribution to existing knowledge.

TECHNICAL NOTES: Information less broad in scope but nevertheless of importance as a contribution to existing knowledge.

TECHNICAL MEMORANDUMS: Information receiving limited distribution because of preliminary data, security classification, or other reasons. Also includes conference proceedings with either limited or unlimited distribution.

CONTRACTOR REPORTS: Scientific and technical information generated under a NASA contract or grant and considered an important contribution to existing knowledge.

TECHNICAL TRANSLATIONS: Information published in a foreign language considered to merit NASA distribution in English.

SPECIAL PUBLICATIONS: Information derived from or of value to NASA activities. Publications include final reports of major projects, monographs, data compilations, handbooks, sourcebooks, and special bibliographies.

TECHNOLOGY UTILIZATION PUBLICATIONS: Information on technology used by NASA that may be of particular interest in commercial and other non-aerospace applications. Publications include Tech Briefs, Technology Utilization Reports and Technology Surveys.

Details on the availability of these publications may be obtained from:

SCIENTIFIC AND TECHNICAL INFORMATION OFFICE

NATIONAL AERONAUTICS AND SPACE ADMINISTRATION

Washington, D.C. 20546